THE INFLUENCE OF THE TESTING MACHINE ON THE BUCKLING OF CYLINDRICAL SHELLS UNDER AXIAL COMPRESSION

by

Charles D. Babcock, Jr.

Graduate Aeronautical Laboratories

California Institute of Technology

Pasadena, California

TABLE OF CONTENTS

DEFINITION OF SYMBOLS

E	Young's modulus
K	testing machine stiffness (lb/in)
K_s	shell stiffness $2\pi RtE/L$
$\overline{K}$	K/K_s
L	shell length
p	load applied to shell
P_{cl}	$\dfrac{p}{2\pi Et^2/\sqrt{3(1-\nu^2)}}$
PE	potential energy
$\overline{PE}$	$PE/\frac{\pi}{4}(\frac{t}{R})^2 ELRt$
PE_s	potential energy of the shell
$\overline{PE}_s$	$PE_s/\frac{\pi}{4}(\frac{t}{R})^2 ELRt$
R	shell radius
t	shell thickness
U_s	strain energy of the shell
$\overline{U}_s$	$U_s/\frac{\pi}{4}(\frac{t}{R})^2 ELRt$
δ	end shortening of shell
δ_{cl}	$tL/R\sqrt{3(1-\nu^2)}$

DEFINITION OF SYMBOLS (cont'd)

$\bar{\delta}$	δ / δ_{cl}
Δ	displacement of loading system
ν	Poisson's ratio
σ	$p/2\pi Rt$
σ_{cl}	$Et/R\sqrt{3(1 - \nu^2)}$
$\bar{\sigma}$	σ/σ_{cl}

THE INFLUENCE OF THE TESTING MACHINE ON THE BUCKLING OF CYLINDRICAL SHELLS UNDER AXIAL COMPRESSION

By Charles D. Babcock, Jr.

SUMMARY

A series of experiments has been carried out on electroformed cylindrical shells under axial compression to determine the effect of the stiffness of the testing machine on the buckling loads. In addition, the effect of the testing machine has been calculated using an energy criterion. It is shown that the calculated energy load has a strong dependence on the testing machine while the experimental data is virtually independent of the testing machine stiffness.

INTRODUCTION

Several authors have carried out investigations on the effect of the method of load application on the buckling loads of shells or other types of structure (Refs. 1 and 2). In particular, one effect that is of interest is the stiffness of the testing machine and how this enters into the determination of the collapse load. For shell structures which have a load deflection curve of the type shown in figure 1, Thompson (Ref. 2) has shown that for infinitesimal disturbances, the effect of the loading apparatus does not enter into the determination of the collapse load. This results from the fact that the initial post buckling state is unstable under all loading conditions. The collapse load will be defined here to be the load at which the shell buckles into the post buckled large deflection state. An experimental confirmation of the fact that the collapse load

is independent of the stiffness of the testing machine will be presented in this paper.

If one considers the effect of finite disturbances on the buckling of shells, the nature of the loading system will be of importance. Unfortunately, the analysis for this type of loading does not exist except for very simple systems with few degrees of freedom. However, the effect of finite disturbances can be assessed very easily if one is willing to use some type of energy criterion. Once the characteristics of the loading apparatus and the loaded shell are known, the buckling load can be calculated. This will be done for two energy criteria advanced by Tsien (Refs. 1 and 3) and the results compared with the experimental data.

EXPERIMENTAL DATA

Experimental data on the buckling of electroformed cylindrical shells has been obtained during the past several years at GALCIT*. These shells are electrodeposited on wax mandrals. The resulting test specimens have thickness variations of the order of $\pm$ 2 per cent, and have geometrical tolerances of the order of $\pm$ 1/2 t. The initial deformation is measured after mounting the shell in the testing apparatus. During the testing of these shells three different types of loading systems have been used. Each of these will be described briefly.

Testing Machine No. 1

The first type of testing machine was used in the initial phase of all the experimental work and is shown in figure 2. This machine

---

* Graduate Aeronautical Laboratories, California Institute of Technology.

was constructed as a controlled displacement type of machine. The loading is accomplished by the three load screws which have 40 threads per inch. The screws can be turned individually for adjusting the load distribution or simultaneously for increasing the total load. The load is applied to the test cylinder through an intermediate cylinder. This cylinder is instrumented with strain gages which give the load distribution on the test cylinder and the total load applied.

The stiffness of the machine was determined by measuring the deflection of the screws, bearings, and end plates under load. In this manner the machine stiffness, K, was determined to be 500,000 lb. per inch. In addition, the intermediate cylinder with the strain gages has a stiffness of 2,000,000 lb. per inch. The resultant stiffness of the whole loading system then becomes 400,000 lb. per inch if an intermediate cylinder is used on one end and 333,000 lb. per inch if an intermediate cylinder is used on both ends.

Testing Machine No. 2

This testing machine consisted of a simple loading ring as shown in figure 3. The shell was loaded using this ring in a 300,000 lb. testing machine. Assuming the testing machine is very rigid as compared to the load ring, the spring constant of this loading system is 25,000 lb. per inch.

Testing Machine No. 3

This type of testing machine applies the load by means of a pressure diaphragm similar to the method of loading used in a flutter test at GALCIT (Ref. 4). The pressure is fed to a flexible tube that is constrained by the loading fixture and the end ring of the shell. A

drawing of the loading fixture is shown in figure 4. The loading applied by the pressure diaphragm appears to be dead weight except for the stiffness of the tube. This stiffness was measured to be about 600 lb. per inch.

Buckling data

A total of eight shells suitable for comparison have been tested in these three testing machines. Table I shows the dimensions of the shell, the shell spring constant defined to be

$$K_s = 2\pi RtE/L,$$

and the stiffness of the testing device. The buckling load or collapse load is shown in the table and plotted vs. the ratio of test shell to testing device stiffness in figure 5. This figure shows that the buckling load is clearly not dependent on the stiffness of the loading device over 3 order of magnitude.

ENERGY CRITERION

In 1942 Tsien (Ref. 1) postulated what has been commonly called an energy criterion of buckling. As a revision of his original criterion he proposed a second criterion in 1945 (Ref. 3). These energy criteria are based upon a belief that the shell prefers to be in the post buckled rather than in the prebuckled state. The necessary energy for the transition between the two states is assumed to come from the local testing or field environment.

These energy criteria have been widely discussed and has been shown to be inconsistent with some experimental results. In particular, in a series of experiments by Fung and Kaplan (Ref. 5) the energy criterion first proposed by Tsien was shown to give results disagreeing with experiment. The experiment consisted of a series of tests on low arches where the testing method was the same for a wide range of arch geometry. The purpose of this following calculation is to find the buckling load as given by the energy criterion for a range of testing machine stiffness. This calculation will then be compared with the experimental data for shells of roughly the same geometry.

Tsien's First Energy Criterion

The first criterion, as proposed by Tsien, stated that the shell will jump from the unbuckled state to the buckled state if the potential energy of the two states are equal. Tsien calculated this load for the case of a cylindrical shell. The calculation depends upon the type of the testing machine and the post buckled equilibrium states of the shell. Tsien did this calculation for the dead weight and rigid loading cases, using the load deflection relation as calculated by von Kármán and Tsien (Ref. 6). However, the energy load as defined above can easily be calculated for any loading system as depicted in figure 6, once the load versus deflection relation for the shell and the loading system is known.

The potential energy of the system as shown in figure 6 is made up of the strain energy stored in the shell and the strain energy stored in the loading spring. Assuming the loading spring is linear with spring constant K lb/inch, this energy can be calculated to be

$$PE = \frac{1}{2} K(\Delta - \delta)^2 + U_s \tag{1}$$

The strain energy of the shell, U_s, can be calculated from a load versus deflection (p vs δ) graph of the shell as follows:

$$U_s = \int p d\delta \tag{2}$$

Using the p vs δ graph for a cylindrical shell calculated by Almroth (Ref. 7) and shown in figure 1, the strain energy can be calculated and is shown in figure 7. In these figures the following nondimensional quantities have been introduced.

$$\overline{U}_s = U_s / \frac{\pi}{4} \left(\frac{t}{R}\right)^2 ELRt \tag{3}$$

$$\overline{\sigma} = \sigma/\sigma_{cl} = \sigma \Big/ \frac{Et}{R\sqrt{3(1-\nu^2)}}, \quad \overline{\delta} = \delta/\delta_{cl} = \delta \Big/ \frac{tL}{R\sqrt{3(1-\nu^2)}}$$

where $\sigma = \frac{p}{2\pi Rt}$ and Poisson's ratio has been taken to be 1/3. The strain energy of the shell could also be calculated by using the potential energy plot calculated by Almroth and shown in figure 8. This calculation is performed as follows:

$$U_s = PE_s + p\delta \tag{4}$$

In nondimensional form this equation becomes

$$\overline{U}_s = \overline{PE}_s + 3\overline{\sigma}\,\overline{\delta} \tag{5}$$

where

$$\overline{PE}_s = PE_s / \frac{\pi}{4}\left(\frac{t}{R}\right)^2 ELRt \tag{6}$$

Using either figure 7 or 8 the potential energy of the whole system can be calculated for any linear testing machine using the following equations.

$$\overline{PE} = \overline{U}_s + \frac{3}{2}\frac{\bar{\sigma}^2}{\bar{K}} \tag{7}$$

or

$$\overline{PE} = \overline{PE}_s + 3\,\bar{\sigma}\,\bar{\delta} + \frac{3}{2}\frac{\bar{\sigma}^2}{\bar{K}} \tag{8}$$

where

$$\bar{K} = K/K_s = K/\frac{2\pi RtE}{L} \tag{9}$$

These calculations have been carried out for a range of $\bar{K}$ from 10^{-3} to 10^{2} and a buckling load determined based upon the first energy criterion. The results of this calculation is shown in figure 5 and labeled E-1.

Tsien's Second Energy Criterion

The next criterion of buckling that Tsien proposed, was that the shell will jump from the unbuckled state to the buckled state whenever there is an available stable equilibrium position in the post buckled state. However, the availability of such a stable position depends not only on the characteristics of the shell but also on the loading system. If the machine is a dead weight type of machine, then the jump must be

made under constant load and if the machine is a rigid one, the jump must be made under constant displacement. Any linear elastic machine will fall between these two extremes. The load at which this jump will occur can be found from the load deflection curve for the shell by simply drawing the inverse slope of the testing machine on the graph and finding the minimum load for which this line intersects the post buckled range of the shell. The end result of the calculation is shown in figure 5 and labeled E-2. Again, Almroth's load vs deflection relation has been used for this calculation.

CONCLUSION

The results of the experimental work and the calculated energy loads by the two energy criteria are compared in figure 5. The variation of the energy load with testing machine stiffness is similar for both criteria but is always lower for the second. This is due to the fact that, for the second criterion, the system is allowed to jump to a state of higher potential energy.

The comparison with the experimental points shows that an energy criterion of this type does not properly predict the dependence of the buckling load on the testing machine stiffness. As noted before, Fung and Kaplan (Ref. 5) showed that the first energy criterion did not properly predict the dependence of the buckling load on the geometry of the test specimen for the same type of testing machine.

REFERENCES

1. Tsien, H. S.: A Theory for the Buckling of Thin Shells. Journal Aeronautical Science, Vol. 9, p. 373, 1942.
2. Thompson, J. M. T.: Stability of Elastic Structures and Their Loading Devices. Journal of Mechanical Engineering Science, Vol. 3, No. 2, 1961.
3. Tsien, H. S.: Lower Buckling Load in the Non-Linear Buckling Theory for Thin Shells. Quart. Appl. Math., Vol. 5, p. 236, 1947.
4. Olson, M. D.: Supersonic Flutter of Circular Cylindrical Shells Subjected to Internal Pressure and Axial Compression. AFOSR 65-0599, April 1965.
5. Fung, Y. C. and Kaplan, A.: Buckling of Low Arches and Curved Beams of Small Curvature. NACA TN 2840, 1952.
6. von Kàrmàn, T. and Tsien, H. S.: The Buckling of Thin Cylindrical Shells under Axial Compression. Journal Aeronautical Science, Vol. 8, No. 8, p. 302, 1941.
7. Almroth, B. O.: Postbuckling Behavior of Axially Compressed Circular Cylinders. AIAA Journal, Vol. 1, No. 3, March 1963.

TABLE I

EXPERIMENTAL DATA

Shell	L	$tx10^{3}$	R/t	$Ex10^{-6}$	$K_s x10^{-5}$	Testing Machine	K/K_s	σ/σ_{cl}
1	7.0	5.28	760	16.0	3.03	1	1.10	.618
2	8.0	4.41	910	16.0	2.22	1	1.50	.656
3	10.0	4.69	850	16.7	1.97	1	2.03	.687
4	10.0	5.12	790	15.8	2.04	1	1.96	.684
5	8.0	3.91	1020	16.0	1.96	2	$1.28x10^{-1}$	.688
6	8.0	3.46	1160	16.6	1.79	3	$3.35x10^{-3}$	.674
7	8.1	4.16	960	17.2	2.22	3	$2.70x10^{-3}$	.612
8	6.9	4.18	960	16.7	2.53	3	$2.37x10^{-3}$	.655

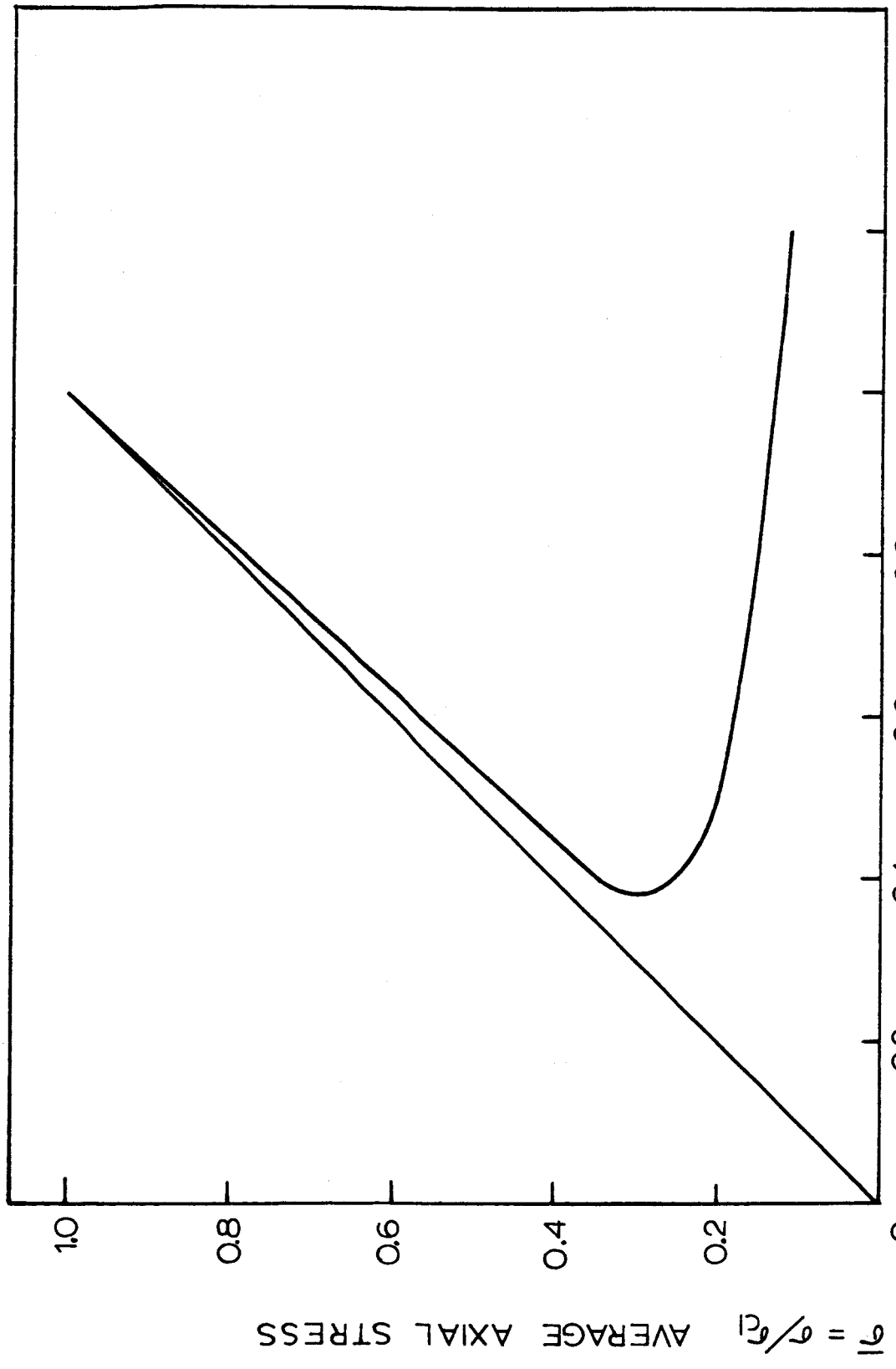
$\bar{\sigma} = \sigma/\sigma_{cl}$ AVERAGE AXIAL STRESS
1.0
0.8
0.6
0.4
0.2
0
0.2
0.4
0.6
0.8
1.0
1.2
$\bar{\delta} = \delta/\delta_{cl}$ SHELL END SHORTENING

FIG. 1

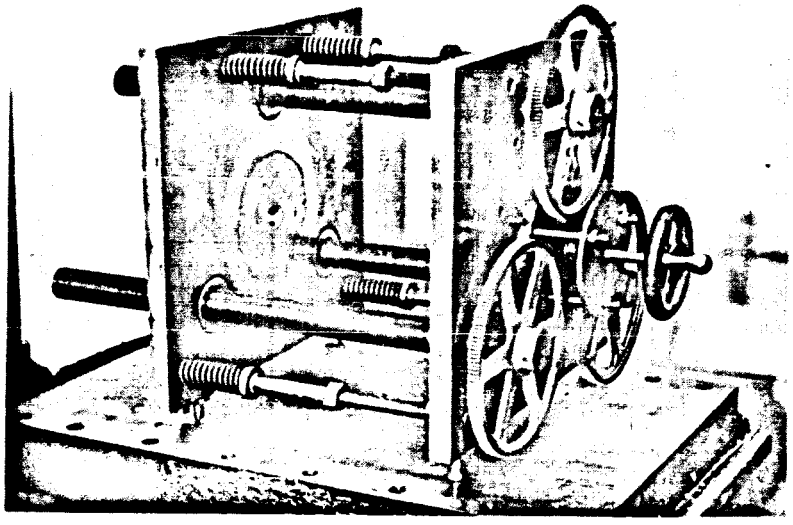

Fig. 2. Testing Machine No. 1, Controlled Shortening Loading.

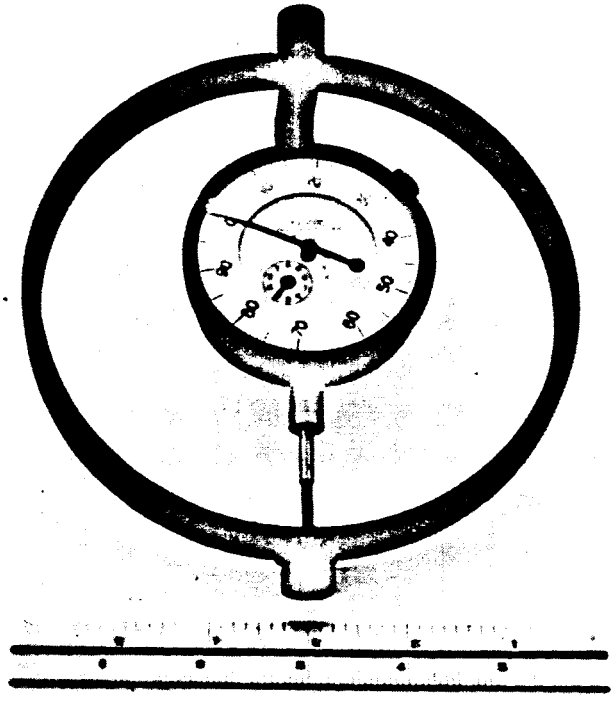

Fig. 3. Testing Machine No. 2, Load Ring.

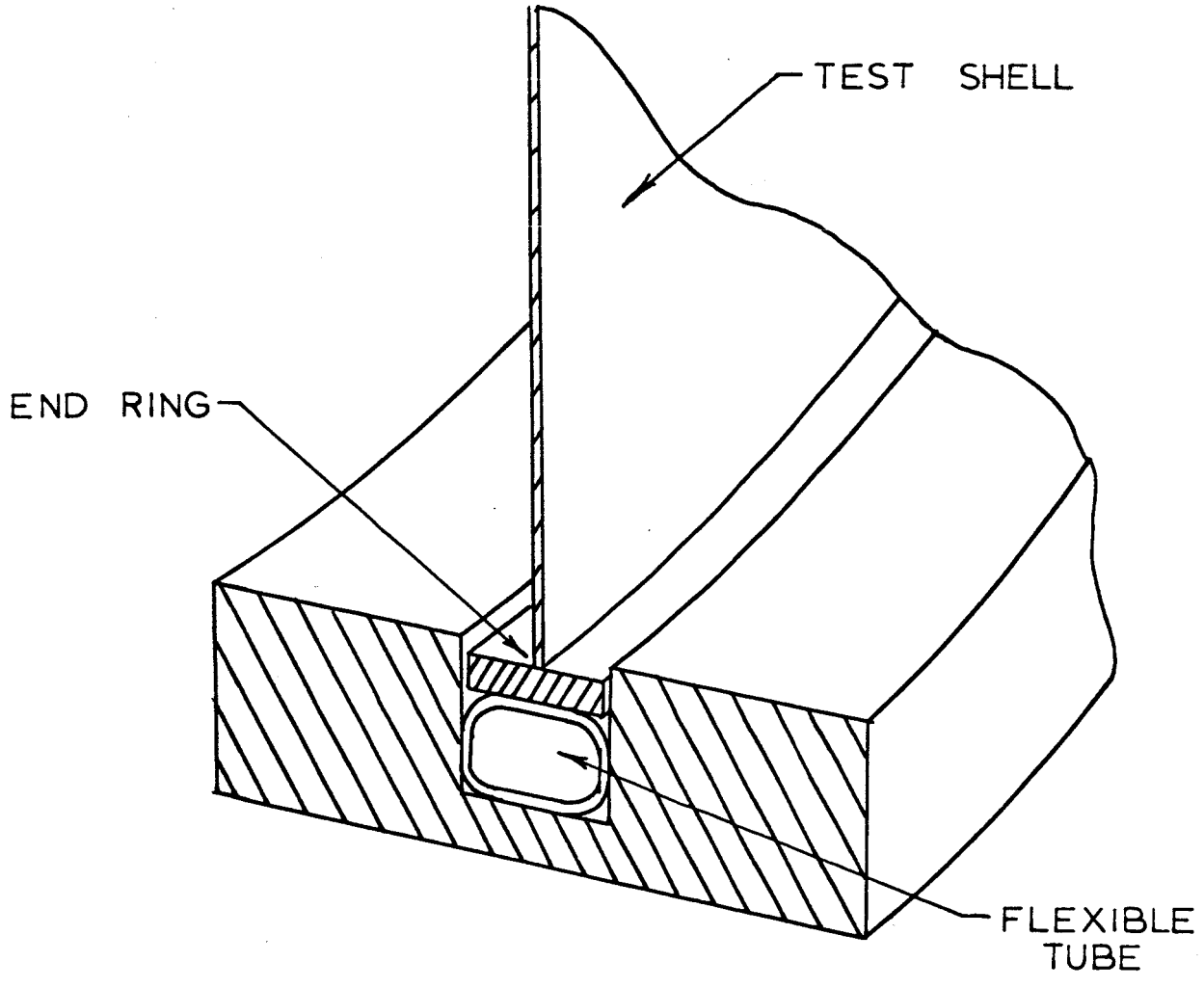

TESTING MACHINE NO. 3
PRESSURE LOADING

FIG. 4

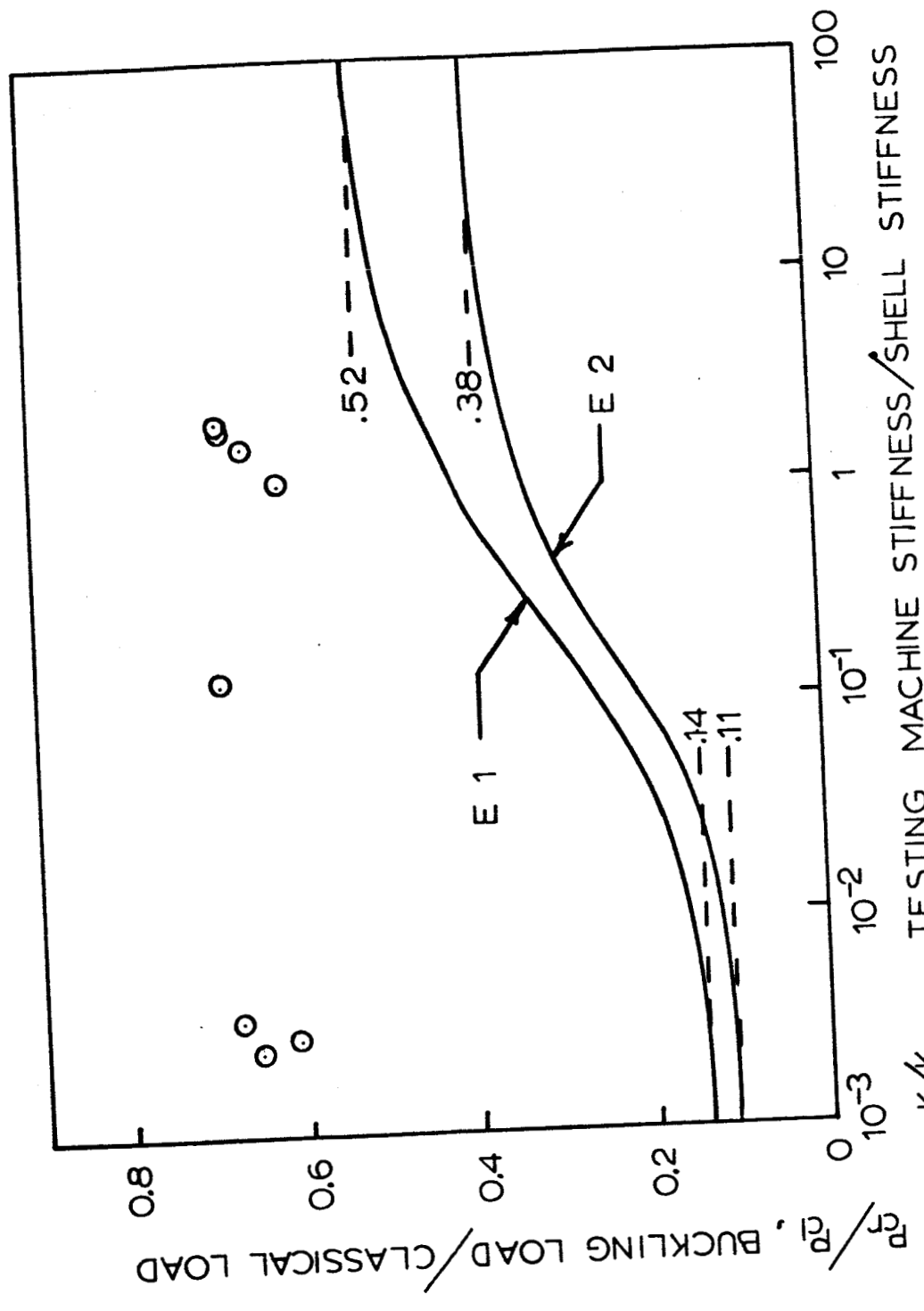
σ_{cr}/σ_{cl}, BUCKLING LOAD/CLASSICAL LOAD
0.8
0.6
0.4
0.2
0
10^{-3}
10^{-2}
10^{-1}
1
10
100
K/K_s, TESTING MACHINE STIFFNESS/SHELL STIFFNESS
.52
.38
.14
.11
E 1
E 2

FIG. 5

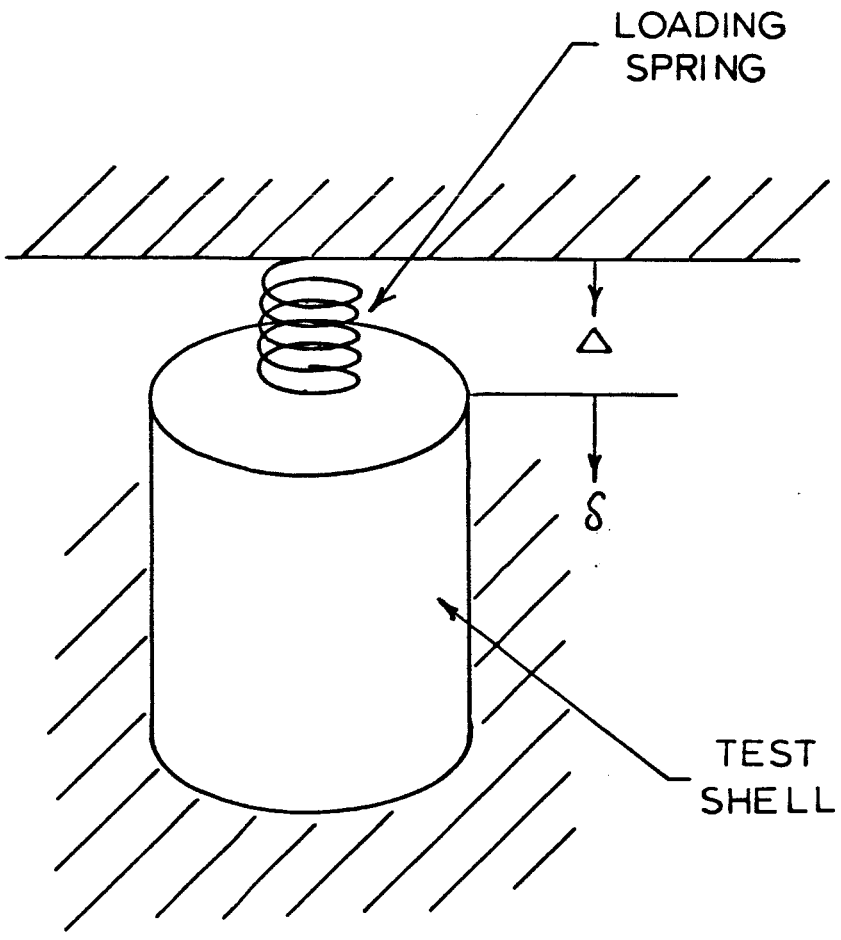

FIG. 6

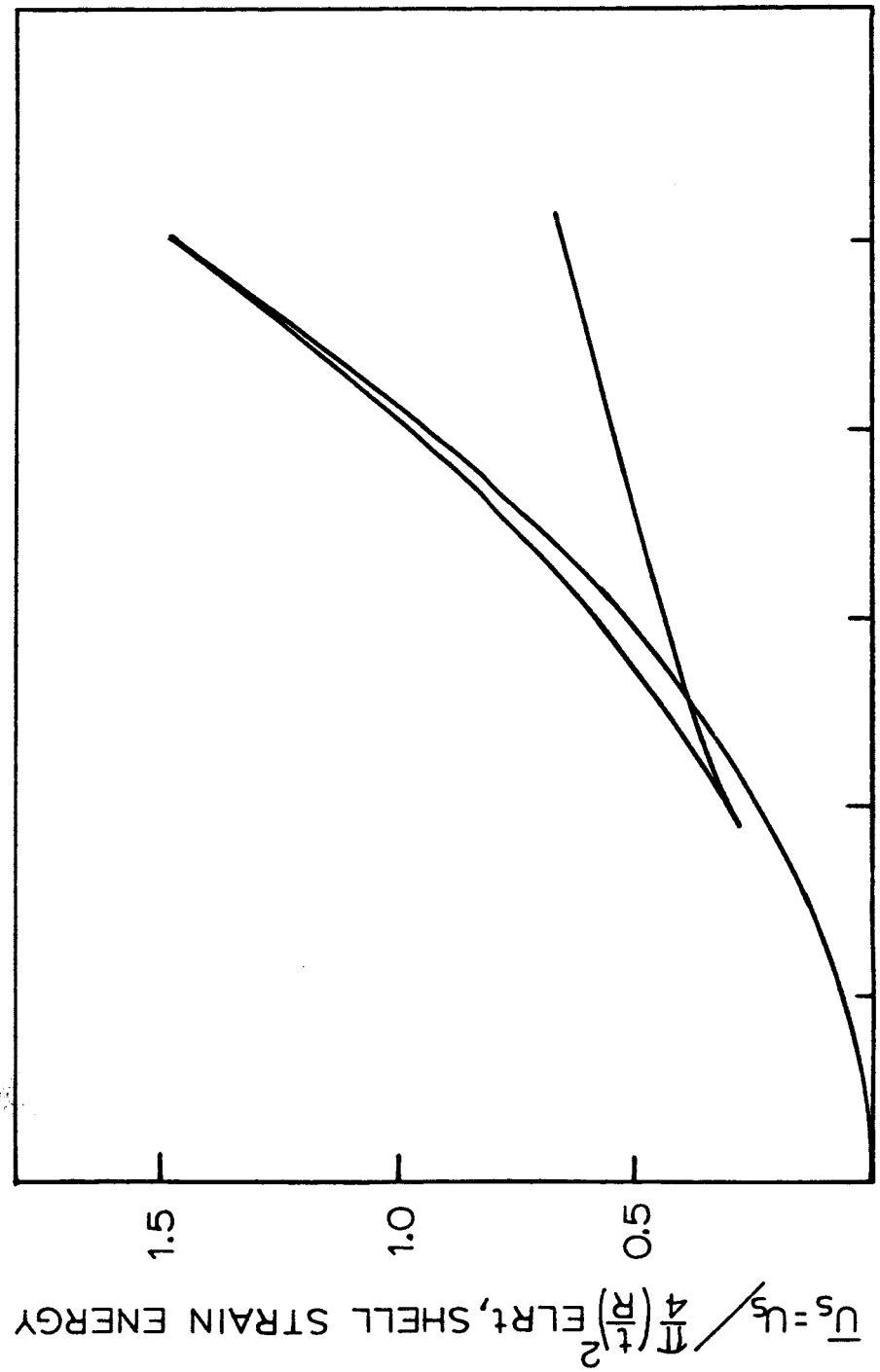
$\overline{U}_S = U_S / \frac{\pi}{4}\left(\frac{t}{R}\right)^2 E L R t$, SHELL STRAIN ENERGY
1.5
1.0
0.5
0
0.2
0.4
0.6
0.8
1.0
$\overline{\delta} = \delta/\delta_{cl}$ SHELL END SHORTENING

FIG. 7

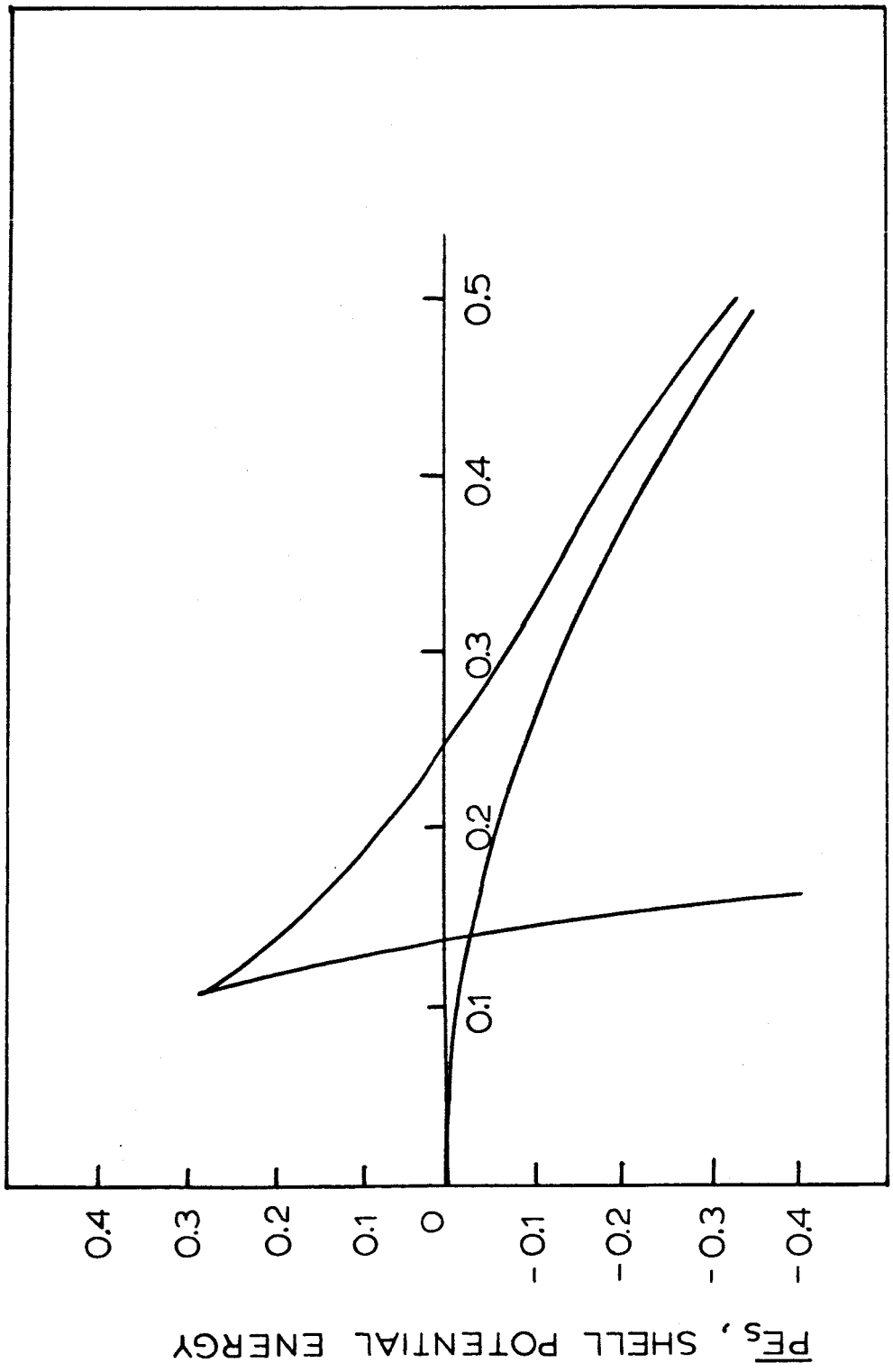
0.4
0.3
0.2
0.1
0
-0.1
-0.2
-0.3
-0.4
0.1
0.2
0.3
0.4
0.5
PEs , SHELL POTENTIAL ENERGY
σ̄ = σ/σCl AVERAGE AXIAL STRESS

FIG. 8